Soft Matter

PAPER

View Article Online
View Journal

Cite this: DOI: 10.1039/c5sm00146c

Droplet–droplet interactions investigated using a combination of electrochemical and dynamic light scattering techniques. The case of water/BHDC/benzene:*n*-heptane system†

Juán Sebastián Florez Tabares, N. Mariano Correa, Juana J. Silber, Leonides E. Sereno* and Patricia G. Molina*

Received 19th January 2015
Accepted 23rd February 2015

DOI: 10.1039/c5sm00146c

www.rsc.org/softmatter

In this contribution the electrochemistry of $[Fe(CN)_6]^{4-/3-}$ as the probe molecule was investigated in benzyl-*n*-hexadecyldimethylammonium chloride (BHDC) reverse micelles (RMs) varying the composition of the external solvent (benzene:*n*-heptane mixtures) and the surfactant concentration, at a fixed water content and probe concentration. The electrochemical and dynamic light scattering results show that in water/BHDC/benzene:*n*-heptane systems the aggregate sizes increase on increasing BHDC concentration. This behavior was unexpected since it is known that for water/BHDC/benzene RM systems keeping the water content constant and the surfactant concentration below 0.2 M, the droplet sizes are independent of the concentration of the surfactant. We explain the results considering that on changing the external solvent to benzene:*n*-heptane mixtures, RMs tend to associate in clusters and equilibrium between free RMs and droplet clusters is established. A model is presented which, using electrochemical and dynamic light scattering data, allows calculating the aggregation number of the RMs, the number of RMs that form the droplet clusters and the standard electron transfer heterogeneous rate constant.

1. Introduction

Reverse micelles (RMs) are formed spontaneously when some surfactants are dissolved in nonpolar organic solvents. These are usually spherical aggregates of surfactant molecules with the outer shell forming the hydrophobic tails while the polar heads form the inner core.[1–3] RMs have been an interesting subject over the past few decades due to their broad applications in chemical reactions, separation science, materials science, and in the pharmaceutical industry, among others.[4–6] There are a wide range of surfactants that form RMs, including anionic, cationic and nonionic molecules.[1–3,7–13] Probably, the anionic surfactant most frequently used to create RMs is sodium 1,4-bis-2-ethylhexylsulfosuccinate (AOT). AOT has a well-known V-shaped molecular geometry, giving rise to stable RMs without a cosurfactant in a variety of nonpolar organic solvents.[1–3,7,9,10,14] One of the most important properties of the AOT RMs is their ability to encapsulate a fairly large amount of water to form a surfactant-coated nanometer-sized water droplet dispersed in a nonpolar liquid. Moreover other polar non-aqueous solvents including ionic liquids[15–19] can also be entrapped in the polar core, forming a polar pool surrounded by a layer of surfactant molecules dispersed in the nonpolar pseudophase. Unlike most of the cationic surfactants, benzyl-*n*-hexadecyl dimethylammonium chloride (BHDC) also forms RMs in aromatic solvents without the addition of a cosurfactant and has properties that are characteristic of other RM systems. They can encapsulate water in their polar interior, and in benzene for example water is solubilized up to W_0 = [water]/[BHDC] around 25, and the size of the RMs increases with increasing water content.[20–25]

It is known that the properties of RMs depend on the type of surfactant and the W_0 values,[1–4,12,24,25] but the influence of the non-polar organic pseudophase has been less examined. Most of the studies on the subject were performed on the anionic AOT RM system,[7,8,26–29] and only few studies are found for cationic RM media.[21,30]

An interesting approach that was first reported to vary the properties of AOT RMs is the use of solvent mixtures.[31–33] Thus, it was demonstrated that it is possible to control the stability of the RMs by applying mixtures of "good" and "bad" solvents to create microemulsions. The concept of "good" and "bad" solvents was used for those solvents that "switch off

Departamento de Química, Universidad Nacional de Río Cuarto, Agencia Postal # 3, X5804ALH, Río Cuarto, Argentina. E-mail: pmolina@exa.unrc.edu.ar; lsereno@exa.unrc.edu.ar; Fax: +54-358-4676233; Tel: +54-358-4676233

† Electronic supplementary information (ESI) available: Fig. S1: Dependence of i_L/r_d4F ratio with [surfactant] for AOT and BHDC RMs. See DOI: 10.1039/c5sm00146c

(decreased)" or "switch on (increased)" the attractive interdroplet interactions, respectively.[31–33]

On the other hand, while droplet interaction plays a predominant role in the size control of the RMs, the nature of the RM interfaces has to be relevant because mass transfer is not possible unless the interface is ruptured in some way.[29] In this sense, we decided to investigate the effect that external nonpolar solvent blends may have on both the BHDC interdroplet interactions and the BHDC RM interface properties within the reversed micellar stability region of the phase diagram.[34] We observed that the maximum W_0 decreases as the *n*-heptane content increases and that the amount of water decreases dramatically at X_{HP} (where X_{HP} is the *n*-heptane mole fraction) above 0.13. It must be noted that BHDC is a surfactant that cannot be dissolved and does not form RMs in saturated hydrocarbons. Also we found that $X_{HP} = 0.59$ is the maximum amount of *n*-heptane that can be added to the system producing optically clear solution. After that, the system collapses (phase transition). Therefore, benzene plays a major role in the RM stabilization. To find out the size and properties of the interface we studied water/BHDC/benzene:*n*-heptane RMs using dynamic light scattering (DLS) and the solvatochromism of 1-methyl-8-oxyquinolinium betaine (QB) at a fixed temperature.[34] We demonstrated that the BHDC RM sizes and interfacial composition change upon *n*-heptane addition, as it was previously shown for AOT RMs with a nonpolar phase blend.[31] Thus, for BHDC RMs formed in benzene:*n*-heptane mixtures, droplet sizes, interfacial micropolarity and the water–polar head surfactant interaction increase as the *n*-heptane content increases. These results suggest that, as the *n*-heptane mole fraction increases, the interdroplet interaction also increases making the RM droplet size larger, increasing the overlapping between droplets accompanied by removal of benzene from the interface.[35–37]

We have previously shown that electrochemical measurements can be a powerful alternative approach to investigate RMs[38] and other organized media.[39,40] Thus and considering that RMs are useful for membrane mimetic studies where the electron-transfer process is important,[41] we decided to study the effect of the micellar interface and solvent blends on BHDC RMs by electrochemical methods using $[Fe(CN)_6]^{4-/3-}$ as the probe. We have previously studied this redox couple in water/AOT/*n*-heptane RMs[38] on a Pt microelectrode. $[Fe(CN)_6]^{4-/3-}$ behaves unexpectedly inside the AOT RMs. At low concentrations of AOT $[Fe(CN)_6]^{4-/3-}$ undergoes ion pairing with K^+ counterions producing electroinactive associated species. The association process is favored when the molecular probe occupation number is greater than 2 because of the low water availability for ion solvation. As the water content increases, the ion solvation increases and reduces the degree of association producing $[Fe(CN)_6]^{4-/3-}$ which resides in the water pool where the electrochemical response is close to the one obtained in water for the non-associated species. We develop a model to interpret the data which allowed us to calculate the real concentration of the electroactive species, the one that is not associated with the K^+ counterions, the AOT RMs diffusion coefficient, and the micellar hydrodynamic radius. The values are in very good agreement with results obtained by other techniques which clearly show that electrochemical measurements are a good alternative to show effects in these types of media that sometimes are not detected by other common techniques.

In this contribution the electrochemistry of $[Fe(CN)_6]^{4-/3-}$ as the probe molecule was investigated in BHDC RMs varying the composition of the external solvent (benzene-*n*-heptane mixtures), the surfactant concentration keeping W_0 and the probe concentration constant in order to gain insights into how the external solvent blend affects the droplet–droplet interaction, a process that is crucial for nanoparticle synthesis using reverse micelles as the nanotemplate. An unusual behavior was observed in the limiting current, i_L, as a function of BHDC concentration which suggested association of RMs into clusters, a result that is not easy to explain and quantify with techniques such as spectroscopy and dynamic and static light scattering. A quantitative model was developed to determine the relationship between RMs and the observed droplet clusters in equilibrium. In this sense, this study pursues three main goals: (i) to explore the influence of the charge in the surfactant polar heads on the electron-transfer reactions; (ii) to estimate the aggregation number of BHDC molecules in the RMs not yet known under these conditions; (iii) to obtain information about the behavior of the droplet–droplet interactions. We want to emphasize that we used electrochemical methods to the system water/BHDC/benzene:heptane to unravel the unusual interdroplet interactions that we observed using molecular probes and dynamic light scattering. In fact the unexpected value of the limiting current observed in the system led us to propose the aggregation of RMs into clusters. The fact that the RMs of the system studied aggregate into clusters when the concentration of BHDC is increased precludes the use of other techniques. The usual techniques to determine aggregation number, for example static light scattering or fluorescence quenching, require changing the surfactant concentration upon the assumption that the properties of the RMs are unchanged and only the concentration of the RM increases, which clearly did not happen in our system. Also, our results give new insights into droplet–droplet interactions which are the key for nanoparticle synthesis using RMs as nanotemplates, an avenue that we are currently investigating.

2. Experimental section

2.1 Materials

Benzene and *n*-heptane both from Merck, HPLC grade, were used without further purification. Benzyl-*n*-hexadecyl-dimethylammonium chloride (BHDC) from Sigma (>99% purity) was recrystallized twice from ethyl acetate. BHDC was dried under reduced pressure, over P_2O_5 until constant weight was achieved.[8] Sodium 1,4-bis(2-ethylhexyl)sulfosuccinate (AOT) from Sigma (99%) was used as received. It was kept under vacuum over P_2O_5. Ultrapure water was obtained from Labconco equipment model 90901-01. All other reagents were analytical grade and used without purification.

2.2 Methods

The benzene solutions and benzene:*n*-heptane mixtures studied were prepared by volume.

The stock solutions of BHDC in the benzene:*n*-heptane mixture and AOT in benzene:*n*-heptane mixtures were prepared by weight and volumetric dilution. To obtain optically clear solutions they were shaken in a sonicating bath and water was added using a calibrated microsyringe. The amount of water present in the system is expressed as the molar ratio between water and the surfactant (W_0 = [water]/[surfactant]). The electroactive probe $K_4[Fe(CN)_6]$ (Mallinckrodt) was dissolved in water prior to mixing with BHDC or AOT/organic phase. After mixing and sonicating transparent and stable RM solutions were obtained. The concentration of $K_4[Fe(CN)_6]$ was kept constant at 1×10^{-3} M, while the concentration of BHDC was varied between 0.016 M and 0.200 M at $W_0 = 5$. The stability of the solutions without the probe molecule was controlled by dynamic light scattering (DLS) and the solutions were found to be stable during this time, about a week.

2.3 DLS measurements

The apparent hydrodynamic diameters (d_{app}) of the different particles of BHDC aggregates were determined by dynamic light scattering (DLS, Malvern 4700 with a goniometer) with an argon-ion laser operating at $\lambda = 488$ nm. All the measurements were made at an angle of 90° and at a temperature of 25 ± 0.1 °C. The correlation function $g(\tau)$ was analyzed by the CONTIN algorithm. This algorithm provides three types of distribution, by number, volume and intensity.[42] The distribution by number was used since it represents the relative percentage of frequencies detected by the spectrophotometer and it allows a detailed quantitative analysis of all the different particles detected. This analysis is necessary to determine the contribution to the limit current for each type of particle (see below). Also a weighted average of the hydrodynamic radius of the particles is obtained, which is very useful for the characterization of the system.

BHDC and AOT solution samples were filtered using an Acrodisc with a 0.2 μm PTFE membrane (Sigma). Viscosities, density, and refractive indices of pure benzene and *n*-heptane, solvent mixtures required for the DLS analyses and X_{HP} calculation, were taken from the literature.[34,43]

2.4 Electrochemical measurement

An AutoLab PGSTAT 30 potentiostat, controlled by GPES 4.8 software, was employed for the linear voltammetry (LV) measurements in conjunction with a Faraday box so that the noise level was in the pA range. The working electrode was a Pt microelectrode obtained from BAS which was polished with 1 μm diamond powder, sonicated, copiously rinsed with distilled water and dried prior to use until reproducible surfaces were obtained. The microdisc electrode radii (r_d) were calibrated using the well-known limiting current expression[44] given in eqn (1):

$$i_L = 4nFr_dDC^* \quad (1)$$

where i_L is the limiting current (A), n is the number of electrons transferred per molecule reacting, F is Faraday's constant (C mol^{-1}), D is the diffusion coefficient of $[Fe(CN)_6]^{4-/3-}$ (cm^2 s^{-1}), C^* is the bulk concentration in mol cm^{-3} and r_d is the disk radii in cm. The disk radius r_d was determined prior to each experiment in the micellar media by recording linear voltammograms in aqueous solutions of known concentrations of $K_4[Fe(CN)_6]$ in 0.5 M KNO_3 at 25 °C using a value of D for $[Fe(CN)_6]^{4-/3-} = (7.56 \pm 0.1) \times 10^{-6}$ cm^2 s^{-1}.[45] The r_d values were between 2×10^{-5} cm and 5×10^{-5} cm.

The counter electrode was a Pt foil (approx. 0.125 cm^2 area). A freshly prepared Ag/AgCl quasi-reference electrode was used; the potentials were corrected for *iR* drop by positive feedback techniques. All the experiments were performed under a purified nitrogen atmosphere. For comparison purposes the current values are referred to the same radius of the electrode. All measurements were carried out at 25 ± 0.1 °C.

OriginPro 7.0 was used for analysis and calculations.

2.5 Processing the steady-state voltammograms

The redox reaction studied is shown in eqn (2). This equation allows us to explore the dynamics of the micellar media and determine how the electron transfer process is affected by the presence of the charged interface.

$$[Fe(CN)_6]^{4-} \rightleftarrows [Fe(CN)_6]^{3-} + 1e^- \quad (2)$$

Steady-state current (i) *vs.* potential (E) curves were recorded at low scan rates (10 mV s^{-1}) with the purpose of assuring the steady-state condition.[46] Five of these curves, all under the same experimental conditions, were averaged previously to proceed with further corrections. These curves were reproducible around ±5%. Steady-state curves are broadened by the ohmic drop effect, (iR_{oh}). In order to obtain the best *i*–*E* curves, the experimental curves were corrected for base line and ohmic drop. The base line was subtracted, taking the tangents to the *i*–*E* curves far from the current response of the redox couple.

The ohmic drop was corrected by positive feedback techniques using the program of the instrument. This procedure was used in each of the BHDC RM media studied.

3. Results and discussion

3.1 Selection of the best external solvent mixture

Initially we searched for the appropriate nonpolar organic solvent to form BHDC RMs and allow observation of the electrochemical discharge of $[Fe(CN)_6]^{4-}$. On the premise that a certain amount of water is necessary to solvate $[Fe(CN)_6]^{4-}$ ions to observe their oxidation, the required solvent should yield a relatively high W_0 value. In pure benzene, BHDC forms RMs accepting water up to $W_0 = 25$;[24,25] however, no electrochemical response was obtained for $[Fe(CN)_6]^{4-}$ in this medium. Since we have successfully studied this probe previously in AOT/*n*-heptane RMs[38] and as BHDC is not soluble in *n*-heptane, we tried electrochemical experiments on $K_4[Fe(CN)_6]$ in AOT/benzene RMs under the same experimental conditions used for BHDC/benzene RMs. Unexpectedly, we did not obtain any

electrochemical response concluding that the external solvent is a determinant factor in the electrochemical response of $K_4[Fe(CN)_6]$.

Knowing that properties such as the external solvent and water penetration and micropolarity of the RMs change with the composition of the external solvent,[34,36,37] we performed electrochemical studies in different benzene:*n*-heptane mixtures, in order to find out the best solvent blend for optimum electrochemical response.

Fig. 1 shows linear voltammograms of $K_4[Fe(CN)_6]$ in the water/BHDC/benzene:*n*-heptane media keeping [BHDC], $K_4[Fe(CN)_6]$ and W_0 constant and varying the blend composition of the benzene and *n*-heptane mixture.

In a previous study we showed that the maximum amount of water that BHDC RMs in benzene:*n*-heptane can accept forming stable and transparent solutions is $W_0 = 5$.[34] Thus, herein $W_0 = 5$ was chosen for the different mixtures studied. As can be seen in Fig. 1, the electrochemical response is favored with the addition of *n*-heptane to the RMs. In the inset of Fig. 1 it is shown that the limiting current (i_L) reaches a maximum value for a 70 : 30% v/v benzene:*n*-heptane blend (which means $X_{HP} = 0.21$).[34,43] For mixtures containing a greater amount of *n*-heptane the system accepts a very limited amount of water because the droplet–droplet interaction is dramatically enhanced.[34] Thus, for reliable and reproducible electrochemical measurements it is necessary to have a W value of at least 4.

On the other hand, the fact that only adding a certain amount of *n*-heptane triggers an electrochemical response of the probe seems to indicate that in BHDC RMs there are some interfacial changes in comparison with AOT RMs. We know[34,36,37] that on increasing the *n*-heptane content the surfactant packing parameter decreases, benzene molecules are expelled from the RM interface decreasing the effective interfacial volume and the BHDC interface is richer in interfacial water. Therefore, this enriched RM interface favors the oxidation of the molecular probe.

Moreover, the electrochemical discharge of $[Fe(CN)_6]^{4-}$ was investigated using water/AOT/benzene:*n*-heptane (70 : 30% v/v) RMs at $W_0 = 5$ and [AOT] 0.1 M. Under these conditions no electrochemical signal was observed from the molecular probe which indicates that the anionic AOT interface does not favor the discharge of $[Fe(CN)_6]^{4-}$ even in the presence of *n*-heptane. This result confirms that the nature of the RM interface is crucial for the electron transfer reaction.

Thus, we chose the following experimental conditions: water/BHDC/benzene:*n*-heptane (70 : 30% v/v) at $W_0 = 5$ and $K_4[Fe(CN)_6] = 1 \times 10^{-3}$ M. The BHDC concentration was varied from 0.016 M to 0.200 M.

3.2 DLS results

The concentrations of BHDC used to determine the sizes of the formed droplets were above the critical micellar concentration (cmc) and are the same as those used to obtain the steady-state voltammograms. At [BHDC] = 0.016 M no signal is detected in DLS, while a good electrochemical response is obtained (see below). This result means that the droplets formed at this concentration have sizes close to the detection limit of the instrument and we assume that under these conditions only small isolated RMs are present. Fig. 2 shows the different average apparent diameters (d_{app}) of the droplet distribution as a function of BHDC concentration. The line shows the fit performed on the experimental data with an empirical equation used *a posteriori* to investigate the origin of this distribution. As can be seen, there is an apparent increase in the d_{app} value of the RMs with the surfactant concentration. This is not common in RM media.

The size of the RMs at [BHDC] = 0.016 M in the solvent blend (which could not be measured) was calculated by extrapolation of the DLS data shown in Fig. 2. This gave $d_{app} \cong 1.54$ nm, a value that is within the limits of the sensitivity of our

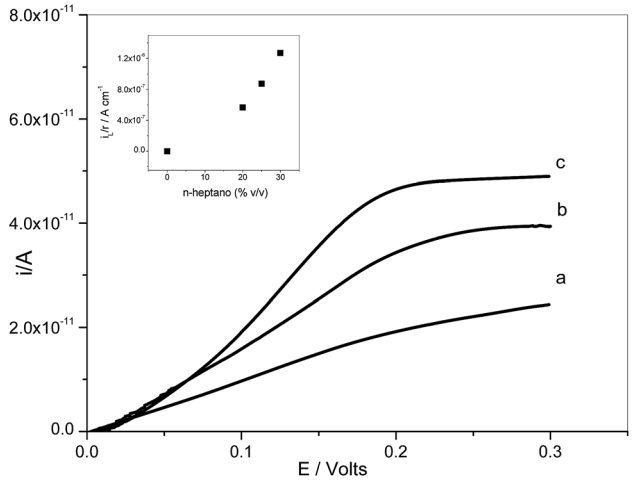

Fig. 1 Current–potential curves for the oxidation of $K_4[Fe(CN)_6]$ 1×10^{-3} M solution in water/BHDC/benzene:*n*-heptane for different mixtures of the external solvent: (a) 80 : 20% v/v, (b) 75 : 25% v/v, (c) 70 : 30% v/v. [BHDC] = 0.1 M, $W_0 = 5$, $v = 0.01$ V s^{-1}. Inset: relationship of i_L/r with composition% v/v *n*-heptane in the mixture for 1×10^{-3} M $K_4[Fe(CN)_6]$ in the water/BHDC/benzene:*n*-heptane system. [BHDC] = 0.1 M, $W_0 = 5$, $v = 0.01$ V s^{-1}.

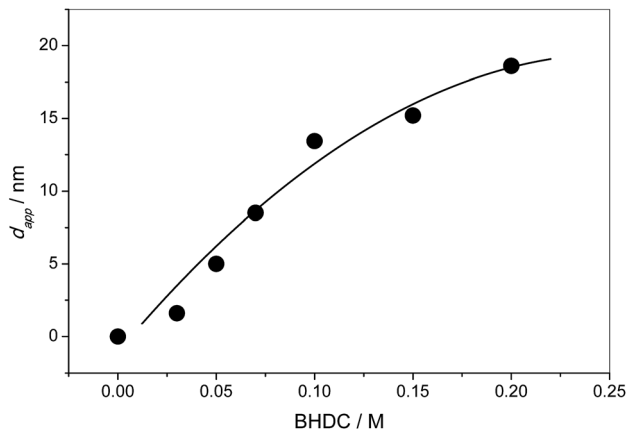

Fig. 2 Diameter dependence of the water/BHDC/benzene:*n*-heptane 70–30% v/v system on [BHDC]. (●) Experimental data obtained from DLS. The line is the fit performed on the experimental data with an empirical equation.

instrument. With this value the RM radius is obtained and by using the Stokes–Einstein equation (eqn (3)), the RM diffusion coefficient is calculated giving a value of $D_M = (4.8 \pm 0.1) \times 10^{-6}$ cm^2 s^{-1} which is within the expected values for the RMs.

$$R_H = \frac{k_B T}{6\eta\pi D} \quad (3)$$

where k_B is the Boltzmann constant, T is the temperature in Kelvin degrees and η is the viscosity of the solvent.[47]

The DLS% distribution frequency number, normalized to one for BHDC concentrations higher than 0.016 M, is shown in Fig. 3. The main feature of these distributions is that they are not symmetrical; all have tails extending to large values of diameter.

Moreover, as the BHDC concentration increases, the width of the distribution also increases. Since we kept the water content constant, $W_0 = 5$, this result is unexpected, because the droplets may increase in number but maintain the same diameter, as usually observed for RMs, as the surfactant concentration increases. The fact that the droplets are increasing in size suggests that the RM droplets are probably assembling into clusters, a result that is odd for RM media and not observed thus far in BHDC/benzene RMs. Thus, in order to explain the results obtained varying the surfactant concentration, we assume that for [BHDC] > 0.016 M the system is composed of isolated RMs and droplet clusters in thermodynamic equilibrium (Scheme 1). It turns out that this equilibrium allows explaining also the electrochemical results as shown below.

3.3 Steady-state voltammograms characterization

The electrochemical response of $K_4[Fe(CN)_6] = 1 \times 10^{-3}$ M in water/BHDC/benzene:*n*-heptane (70 : 30% v/v) RMs varying the BHDC concentration was studied at $W_0 = 5$ and the results are shown in Fig. 4.

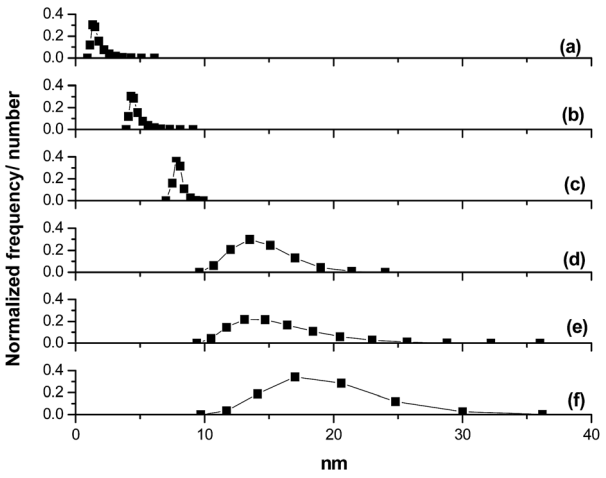

Fig. 3 Normalized frequency number (-■-) as a function of size distributions from the DLS technique in the systems formed in the mixture benzene:*n*-heptane 70–30% v/v $W_0 = 5$ for different [BHDC]: (a) 0.030 M, (b) 0.050 M, (c) 0.070 M, (d) 0.100 M, (e) 0.150 M, (f) 0.200 M.

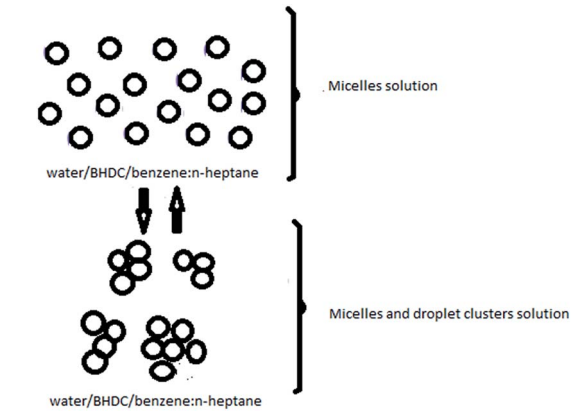

Scheme 1 General diagram illustrating the formation of aggregates of the water/BHDC/benzene:*n*-heptane system.

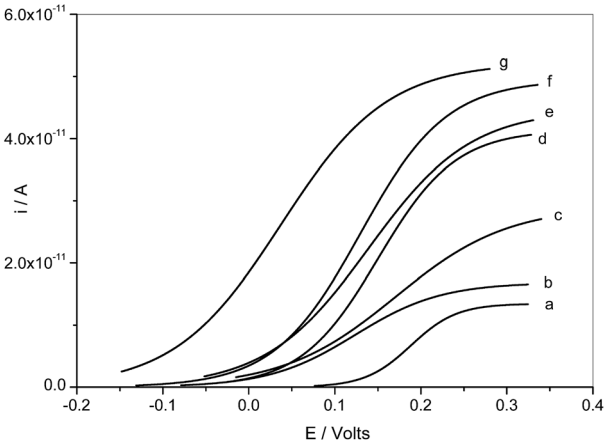

Fig. 4 Experimental current–potential curves for the oxidation of $K_4[Fe(CN)_6]$ 1×10^{-3} M solution in the water/BHDC/benzene:*n*-heptane 70 : 30% v/v system for different [BHDC]: (a) 0.016 M, (b) 0.030 M, (c) 0.050 M, (d) 0.070 M, (e) 0.100 M, (f) 0.150 M and (g) 0.200 M. $W_0 = 5$, $v = 0.01$ V s^{-1}.

In every case well defined waves are obtained and the limiting current (i_L) increases with BHDC concentration. The half-wave potential, ($E_{1/2}$), shifts to more negative values when the concentration of BHDC increases, which means that the environment of the redox couple is changing. To explain this effect we have to consider that for a microelectrode $E_{1/2}$ is defined by eqn (4):[46]

$$E_{1/2} = E_f^o + \frac{RT}{nF} \ln \frac{D_R}{D_O} \quad (4)$$

where E_f^o is the formal redox potential of the species under conditions in which they are dissolved, F is the Faraday constant, 96 484 C mol^{-1}, R is the gas constant in J mol^{-1} K^{-1}, $T = 298$ K and n the number of electrons exchanged by the redox couple. D_R and D_O are the diffusion coefficients of species reduced and oxidized respectively.

Since in our case, the redox couple resides in the RMs, the diffusion coefficient corresponds to the RMs. Then $D_R = D_O$ and

therefore $E_{1/2} = E_f^o$. Another important fact to be noted is the range of potential of the polarization curve that should be taken from the beginning of the curve ($i \cong 0$) to the value of i_L. Normally polarization curves for a reversible system (Nernstian) have a range of 0.160 V, while those for a quasi-reversible system have a much greater range.[48] As can be seen in Fig. 4 the polarization curve corresponding to BHDC = 0.016 M has a reversible behavior, while the other concentrations studied are clearly quasi-reversible. Considering that the concentration of the electroactive species is constant, no changes were expected in the experimental i_L; however, we can see that i_L increases with increasing BHDC concentration.

Quantitative analysis of the two types of polarization curves was performed. The experimental data of the reversible polarization curve corresponding to [BHDC] = 0.016 M were analyzed with the theoretical equation for an anodic reversible process in steady-state shown in eqn (5):[46]

$$\frac{i}{i_L} = \frac{e^{\frac{nF}{RT}(E-E_f^o)}}{1 + e^{\frac{nF}{RT}(E-E_f^o)}} \quad (5)$$

where E is the electrode potential, E_f^o has the same meaning defined above. A non-linear regression of the experimental data with eqn (5) is shown in Fig. 5A. The values of $E_f^o = 0.188$ V and $n = 1$ were obtained.

For BHDC concentrations higher than 0.016 M the systems behave as quasi-reversible. The theory for a quasi-reversible reaction developed for a micro-electrode operating in the steady state regime (eqn (6))[49] was used for the polarization curves for [BHDC] > 0.016 M:

$$\frac{i}{i_L} = \frac{1}{\frac{4D_R}{\pi r_d k_0} e^{(\alpha-1)\frac{nF}{RT}(E-E_f^o)} + \frac{D_R}{D_O} e^{-\frac{nF}{RT}(E-E_f^o)} + 1} \quad (6)$$

where k_0 is the standard heterogeneous rate constant, r_d is the electrode radius and α is the transfer coefficient of the anodic reaction. The value of D_R, the diffusion coefficient of the RMs where the redox couple resides, is obtained as an average of the values calculated by DLS measurements of the same solutions. The other terms have the same meaning as in eqn (5). Typical results are shown in Fig. 5B–D. The nonlinear regression applied to the experimental voltammograms using eqn (5) gives a very good correlation, assuming $n = 1$ in all cases, and allows us to calculate the E_f^o, α and k_0 values which are summarized in Table 1. The value of $\alpha \cong 0.5$ is expected for an electrochemical process where the redox components involved have a very similar structure such as $[Fe(CN)_6]^{4-}/[Fe(CN)_6]^{3-}$. However, the values obtained for E_f^o and k_0 need further explanation. E_f^o gives the wave position and consequently reflects the free energy dependence of the electrode reaction. In our case a shift towards less positive potentials of these values as BHDC concentration increases indicates, from the thermodynamic point of view, that the redox process becomes more favorable. Furthermore since k_0 decreases with increasing BHDC concentration the overall electron transfer process is increasingly slower.

Additionally, since the redox couple resides within the RMs or the droplet clusters (Scheme 1) we may expect several electroactive centers, that is, the electroredox response coming from molecular probes located in different aggregates, each of them interchanging only one electron. The results show that the current–potential response has the same shape as that obtained with the corresponding redox molecule containing only a single center (Fig. 5A where $n = 1$ was assumed). Thus, they behave as non-interacting redox centers.[50] Only the magnitude of the current is enhanced by the presence of additional electroactive centers. This supports the value of $n = 1$ that has been used in all calculations of regression.

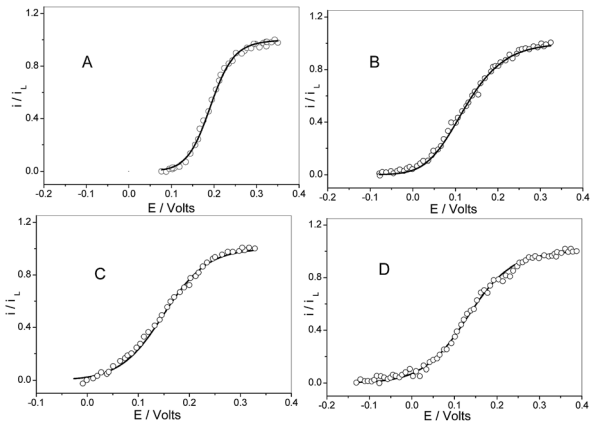

Fig. 5 Experimental i/i_L–potential curves for the oxidation of $K_4[Fe(CN)_6]$ 1×10^{-3} M solution in water/BHDC/benzene:*n*-heptane 70 : 30% v/v at [BHDC] (○) (a) 0.016 M, (b) 0.050 M, (c) 0.070 M, (d) 0.150 M. The line is the theoretical curve obtained for eqn (5) for curve (A) and eqn (6) for (B–D).

3.4 Limiting current interpretation

Fig. 6 shows the behavior of the limiting currents normalized to the $4Fr_d$ parameter (eqn (1)) common to all experiments, for each BHDC concentration studied. In this graph only the first experimental point represents a solution of free RMs, the remaining points are considered to be free RMs and droplet clusters in equilibrium. Hence, to explain the whole behavior of i_L values as a function of BHDC concentration, a theoretical model was developed. This model takes into consideration that the i_L values have two contributions: i_L from free RMs and i_L from droplet clusters.

Table 1 Parameters obtained from the adjustment of the different voltammograms to different [BHDC] with eqn (6)

[BHDC]/M	E_f^o/V	k_0/cm s^{-1}	α
0.030	0.075	0.0390	0.53
0.050	0.073	0.0080	0.57
0.070	0.058	0.0037	0.41
0.100	0.032	0.0030	0.52
0.150	−0.010	0.0012	0.51
0.200	−0.060	0.0017	0.55

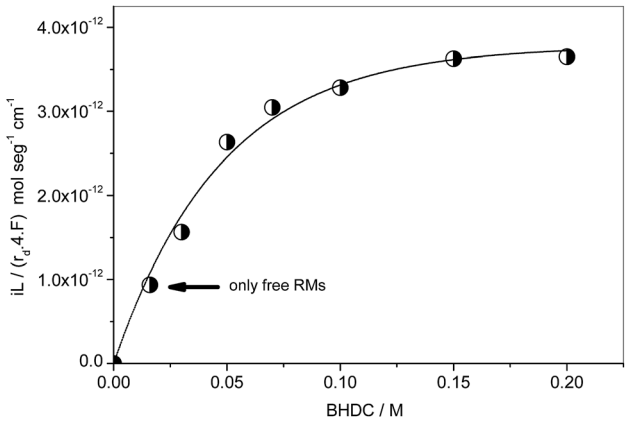

Fig. 6 Relationship between i_L/r_d4F and [BHDC] in the water/BHDC/benzene:*n*-heptane 70 : 30% v/v system, $W_0 = 5$. $[K_4[Fe(CN)_6]] = 1 \times 10^{-3}$ M, $v = 0.01$ V s^{-1}.

3.5 Model and calculations

The model essentially comprises two parts: (a) solution of free RMs and (b) solutions of RMs and droplet clusters in equilibrium (Scheme 1).

The following fundamental assumptions were considered in order to develop the model:

(1) The RMs are assumed to be spherical and equal in size independent of the surfactant concentration.

(2) All the RMs have the same properties, for example the same aggregation number (N_{agg}) of surfactant molecules but this number is yet unknown.

(3) $K_4[Fe(CN)_6]$ resides exclusively inside the RMs, hence random type Poisson distribution can be applied.[51] This distribution foresees RMs with 1, 2, …, j molecules of $K_4[Fe(CN)_6]$, however, which are the active RMs that contribute to the current has to be determined.

(4) The concentration of RMs with (i) molecules inside (denoted by the acronym [MP_i]) is expressed in moles cm^{-3}, according to eqn (1).

(5) The RM droplets can form clusters through the droplet–droplet interaction but retain their identity in the cluster. Also, the formation of clusters is independent of the number of probe molecules inside the RMs.

(6) RMs and droplet clusters are in thermodynamic equilibrium.

(7) The droplet clusters are supposed to be spherical and their size distribution is determined by DLS for each BHDC concentration.

3.5.1 Determination of the aggregation number (N_{agg}). As inferred from the fundamental assumptions listed above, the first step is to determine N_{agg} of the RMs. This is a key point since the experiments needed to determine this parameter require changing the surfactant concentration under the assumption that N_{agg} is independent of the surfactant concentration. As shown in Fig. 2, the aggregate size depends on BHDC concentration and it is not possible to use conventional techniques such as emission spectroscopy and static light scattering. Thus, determination of N_{agg} from our electrochemical and DLS data is mandatory, an approach that, to the best of our knowledge, was not attempted before. We will start the calculation with three known facts: (i) at [BHDC] = 0.016 M the solution is formed only by free RMs; (ii) for this BHDC concentration $i_L/4Fr_d = 1.04 \times 10^{-12}$ mol s^{-1} cm^{-1} (Fig. 6) and; (iii) the diffusion coefficient of the micelles $D_M = (4.8 \pm 0.1) \times 10^{-6}$ cm^2 s^{-1} (calculated in Section 3.2).

Rearranging eqn (1), eqn (7) is obtained:

$$\frac{i_L}{4Fr_dD_M} = nC_{exp} \quad (7)$$

Please note that this equation has a different interpretation from the one used for a solution where the electroactive species is a molecule. Now the meaning of the parameters is as follows: D_M is the diffusion coefficient of the RMs and C_{exp} is the concentration of active RMs. Since the Poisson distribution is applicable, then there are RMs with different numbers of $[Fe(CN)_6]^{4-}$ molecules inside; n is the number of electrons exchanged per RM, so if the active micelle has two molecules of $[Fe(CN)_6]^{4-}$ inside then n will be two and so on. Accordingly, nC_{theo} can be expressed as eqn (8):

$$nC_{theo} = \sum_{i=1}^{i=j}(i[MP_i]) \quad (8)$$

where C_{theo} is electroactive RM concentration, [MP_i] is the RM concentration having "i" $[Fe(CN)_6]^{4-}$ molecules; therefore i is the number of electrons exchanged by these micelles since each molecular probe exchanges only one electron.

According to eqn (7) and taking into account our experimental data, it is possible to calculate nC_{exp} for free RMs, that is for [BHDC] = 0.016 M. The result gives $nC_{exp} = (1.04 \times 10^{-12}/D_M) = 2.16 \times 10^{-7}$ mol cm^{-3}.

Then, the procedure is as follows: it is assumed that N_{agg} is a number between 20 and 110 taking into consideration the values corresponding to BHDC RMs formed in pure benzene.[37] A value of $N_{agg} = 20$ is postulated at first and then the total RM concentration is calculated ($M_t = 0.016/N_{agg}$)^2; with the Poisson distribution[38] the concentration of the different RMs is calculated, [MP_i], and with eqn (8) nC_{theo} is calculated. The sum is from $i = 1$ to a value of j that predicts better agreement with nC_{exp} (eqn (7)), the error is calculated as ($nC_{exp} - nC_{theo}$). This procedure is repeated by changing N_{agg} one unit at a time until the minimum error is obtained. The calculation yields $N_{agg} = 66$ and $j = 3$. This means that active RMs are those with 1, 2 or 3 molecules of $[Fe(CN)_6]^{4-}$.

3.5.2 Limiting currents for [BHDC] > 0.016 M. Under these conditions the experimental limiting current provides two contributions: $i_{L(RMs)} + i_{L(droplet\ clusters)}$. The contribution of each one is something that has to be determined at each BHDC concentration. To do this, the experimental values of $(i_L/4r_dF)_{exp}$ (Fig. 6) are considered. Accordingly, the current expressed in eqn (7) can be expressed as eqn (9).

$$\left(\frac{i_L}{4Fr_d}\right)_{exp} = \frac{i_{L(RMs)}}{4Fr_d} + \frac{i_{L(droplet\ clusters)}}{4Fr_d} \quad (9)$$

Substituting into eqn (9) the current value due to RMs (eqn (8)), eqn (10) is obtained:

$$\left(\frac{i_L}{4Fr_d}\right)_{exp} = 10^{-3}D_M\sum_{i=1}^{i=3}(i[MP_i]) + \frac{i_{L(droplet\ clusters)}}{4Fr_d} \quad (10)$$

The factor 10^{-3} is required to express the concentration of RMs in mole cm^{-3} in accordance with eqn (1). It should be noted that the contribution to the current given by RMs in equilibrium with droplet clusters (first term of eqn (10)) is calculated using the same expression as for free RMs but it does not necessarily give the same numerical value. The concentration of each species depends in turn on each BHDC concentration. Therefore applying the mass balance, eqn (11) can be obtained:

$$[BHDC]_0 = [BHDC]_{RMs} + [BHDC]_{droplet\ clusters} \quad (11)$$

where $[BHDC]_0$ is the total concentration of the BHDC, $[BHDC]_{RMs}$ is the BHDC concentration which is able to give free RMs and $[BHDC]_{droplet\ clusters}$ is the BHDC concentration where the RMs are grouped forming different droplet clusters. If eqn (11) is divided by N_{agg} previously determined, an equivalent eqn (12) is obtained in terms of aggregate concentration

$$[M]_0 = [M]_f + [M]_c \quad (12)$$

where $[M]_0$ is the total aggregate concentration, $[M]_f$ is the free RMs concentration and $[M]_c$ is the concentration of RMs that form droplet clusters.

In order to determine at least one term of eqn (11) or (12), we must take into consideration the size distribution provided by DLS (Fig. 3).

For each BHDC concentration, the total aggregated concentration $[M]_0$ is calculated since now N_{agg} is known. The size distribution obtained by DLS at each BHDC concentration (Fig. 3) is analyzed in order to determine each droplet cluster which is identified as (k_i) and its frequency with (f_k). This is illustrated in Fig. 7 only for the droplet clusters formed at [BHDC] = 0.1 M. In this distribution RMs do not appear due to the reasons explained above (see Section 3.5.1), but are present according to eqn (12). In summary, the system for [BHDC] > 0.016 M is composed of RMs and different droplet clusters characterized by f_k, and k_i. As the droplet clusters are assumed to be spherical and composed of RMs all with the same N_{agg}, immediately a question arises. How many RMs form a droplet cluster? In a first approach, the answer depends on the packing density of the RMs. The random arrangement of spheres of equal size is an important topic to represent the structure of a liquid with ideal behavior. Scott recognized that this packing could be applied to liquids[52] and it is known as "*random close packing of spheres*".[53] The main feature of this arrangement is the effective volume occupied by the spheres or packing density (ϕ) that is the ratio of the volume of the spheres to the total volume that they occupy. A series of experiments and more recently different algorithms of simulation conclude that the value of $\phi \cong 0.64$.[54,55] Since, besides liquids, this packing can be

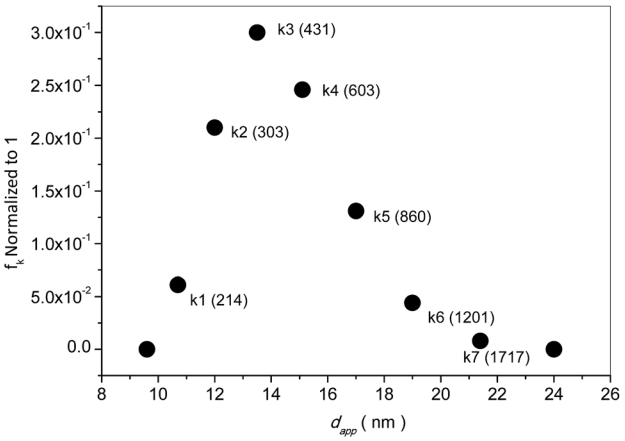

Fig. 7 Normalized frequency (●) as a function of size distributions (diameter, d_{app}) from the DLS technique in reverse micelles formed in the mixture BHDC/benzene:*n*-heptane 70 : 30% v/v W_0 = 5 for [BHDC] = 0.1 M. The number of RMs per droplet cluster, *k*, is indicated in parenthesis for each droplet cluster.

applied to various kinds of particles it is logical to think that it can be used for the packing of the droplet clusters formed by RMs. Accordingly, the number of RMs per droplet cluster *k*, $(NMC)_k$, can be expressed as in eqn (13):

$$(NMC)_k = \frac{\phi \text{Volume droplet cluster } k}{\text{Volume RMs}} = \phi\left(\frac{r_{ck}}{r_M}\right)^3 \quad (13)$$

where r_{ck} is the droplet cluster radius obtained by DLS and r_M is the RM radius.

In Fig. 7 $(NMC)_k$ is indicated between parentheses for each droplet cluster. As discussed before, only a fraction of the RMs contribute to the current, those with i = 1, 2, 3 molecules of $[Fe(CN)_6]^{4-}$. All other RMs do not contribute to the total current.

As the RMs array into droplet clusters randomly, the electroactive fraction can be calculated with eqn (14):

$$f_{MP_i} = \left(\frac{[MP_i]}{[M]_c}\right) \text{ for } i = 1,\ 2,\ 3. \quad (14)$$

where f_{MP_i} is the fraction of electroactive RMs and $[M]_c$ has the same meaning as in eqn (12). The number of RMs of the type MP_i, (i = 1, 2, 3) in each $(\text{droplet cluster})_k$ is given by eqn (15):

$$(\text{RMs Type } i)_k = (\text{NMs})_k f_{MP_i} \quad (15)$$

With this in mind, the number of electrons exchanged per $(\text{droplet cluster})_k$ is shown in eqn (16):

$$n_k = \sum_{i=1}^{i=3} i(\text{RMs Type } i) \quad (16)$$

To calculate the concentration of each droplet cluster, $[\text{droplet cluster}]_k$, the concentration of RMs forming the droplet clusters, $[M]_c$, is divided by $(NMC)_k$ and multiplied by the frequency of each droplet cluster (f_k) provided by DLS data and shown in eqn (17), where the droplet cluster concentration is expressed in moles $liter^{-1}$

$$[\text{droplet cluster}]_k = f_k \frac{[\text{M}]_c}{(\text{NMC})_k} \quad (17)$$

In addition, the mass balance only for droplet clusters at a given BHDC concentration is expressed in eqn (18):

$$[\text{M}]_c = \sum_k [\text{droplet cluster}]_k (\text{NMC})_k = [\text{M}]_c \sum_k f_k \quad (18)$$

Since the frequency has been normalized to one, eqn (19) is valid.

$$\sum_k f_k = 1 \quad (19)$$

Taking into account eqn (16) and (17), the current due to $[\text{droplet cluster}]_k$ is expressed as eqn (20):

$$\left(\frac{i_L}{4fr_d}\right)_k = n_k D_k 10^{-3} [\text{droplet cluster}]_k \quad (20)$$

where D_k is the diffusion coefficient of a given droplet cluster obtained by DLS data. The factor 10^{-3} is required to express the concentration of the cluster in mole cm^{-3} in accordance with eqn (1).

Substituting n_k in eqn (20) and considering eqn (14), (15) and (16), and $[\text{droplet cluster}]_k$ obtained through eqn (17), the following equation is obtained:

$$\left(\frac{i_L}{4fr_d}\right)_k = 10^{-3} D_k f_k \sum_{i=1}^{i=3} i[\text{MP}_i] \quad (21)$$

with all the terms defined above.

The total current due to all the droplet clusters present at any given BHDC concentration is

$$\sum_{k=1}^{k=j} \left(\frac{i_L}{4fr_d}\right)_k = 10^{-3} \left(\sum_{k=1}^{k=j} D_k f_k\right) \sum_{i=1}^{i=3} i[\text{MP}_i] \quad (22)$$

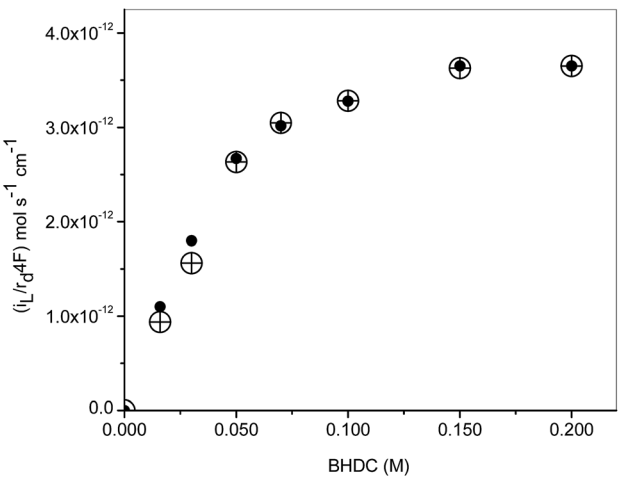

Fig. 8 Comparison of experimental data (●) current with the theoretical values (⊕) calculated with eqn (23).

where j is the total number of droplet clusters for a given BHDC concentration, and is a variable number as may be inferred from Fig. 3.

To obtain the expression for the total current, eqn (22) should be inserted into eqn (10) giving

$$\left(\frac{i_L}{4fr_d}\right)_{\text{theo}} = \left\{10^{-3} D_M \sum_{i=1}^{i=3} (i[\text{MP}_i])\right\}_f + \left\{10^{-3} \left(\sum_{k=1}^{k=j} D_k f_k\right) \sum_{i=1}^{i=3} (i[\text{MP}_i])\right\}_c \quad (23)$$

To evaluate the contribution to the current of each term of eqn (23), eqn (12) must be taken into account at each [BHDC]. Since $[\text{M}]_o$ is known, a tentative value of $[\text{M}]_f \approx 0.016$ is assumed and then $[\text{M}]_c$ is calculated. Thus, with the values of $[\text{M}]_f$ and $[\text{M}]_c$ we proceed to evaluate each term of eqn (23) for each BHDC concentration. The theoretical current is compared with the experimental value $(i_L/4nFr_d)_{exp}$. This iterative procedure is repeated until the error defined as $\{(i_L/4nFr_d)_{exp} - (i_L/4nFr_d)_{theo}\}$ is a minimum. The results of these fits are shown in Fig. 8.

The fits are very good and more important is that a correlation is obtained between the free RM concentrations $[\text{M}]_f$ in equilibrium and those that form droplet cluster $[\text{M}]_c$, as proposed in the model. This correlation is explicitly depicted in Fig. 8.

It is useful to compare the trend in i_L with the surfactant concentration for AOT and BHDC RMs. The variation of i_L/r_d4F with [AOT][38] and [BHDC] is shown in Fig. S1 in the ESI.† As can be seen the i_L/r_d4F values for the discharge of $[Fe(CN)_6]^{4-}$ in the case of AOT RMs are much lower than for the BHDC RMs even though $W_0 = 10$ and the external solvent is pure *n*-heptane for the AOT RM media. This fact clearly shows what was discussed in eqn (8) that, for BHDC RMs media, the experimental i_L has two contributions: i_L (RMs) + i_L (droplet clusters). Besides this, we know that $[Fe(CN)_6]^{4-}$ is located inside the RM droplet and it is probably associated with the positive head of BHDC which is a quite large cation. However, we believe that this association is weak enough for $[Fe(CN)_6]^{4-}$ to be electroactive. Undoubtedly the nature of the association is completely different from the ion pairing of $[Fe(CN)_6]^{4-}$ with K^+ counterions that we have shown previously.[38] This leads to great differences between AOT and BHDC RM systems.

4. Conclusions

In this contribution we were able to show how the external solvent composition is crucial for the interfacial properties of RMs. Thus, we demonstrate that water/BHDC/benzene RMs are discrete non-interacting droplets with an interface where the electron transfer is not a propitious process. On the other hand, the scenario is completely different upon *n*-heptane addition. As we have shown in recent publications[36,37] the fact that benzene molecules are expelled from the interface and water molecules are more involved in the interfacial hydration processes seems to give the ideal conditions for the electrochemical reaction of

the molecular probe. On the other hand, as the *n*-heptane content increases, the droplet–droplet interaction increases and RMs form clusters, resulting in the unusual observation by DLS that the size values are surfactant concentration dependent at fixed values of W_0. We were able to develop a model that allows calculation of the aggregation number of the RMs and the number of RMs that form droplet clusters in equilibrium using a combination of electrochemical and DLS data. Besides, the formal redox potential of the species and the standard electron transfer heterogeneous rate constant at the interface for each [BHDC] were obtained. Although the electron transfer of the probe is thermodynamically a favorable process, it becomes increasingly slower with BHDC concentration. We explain this fact as due to the RM association into clusters which increases the distance of the redox centers to the electrode. Thus, we could interpret the unexpected effect observed in the system studied which is very difficult to detect by other conventional techniques such as emission spectroscopy and static light scattering. This work shows the vast potential of using electrochemical techniques in studying the properties of RM systems. We hope that this contribution will encourage the scientific community to use RMs with a solvent blend as the nanotemplate for nanoparticles with different polydispersities, concentrations and shapes, an avenue that we are currently investigating.

Acknowledgements

We gratefully acknowledge the financial support for this work by the Consejo Nacional de Investigaciones Científicas y Técnicas (CONICET), Agencia Nacional de Promoción Científica y Técnica, and Secretaría de Ciencia y Técnica de la Universidad Nacional de Río Cuarto. N.M.C., J.J.S. and P.G.M. hold a research position at CONICET. J.S.F.T. thanks CONICET for a research fellowship.

Notes and references

1 T. K. De and A. Maitra, *Adv. Colloid Interface Sci.*, 1995, **59**, 95.
2 J. J. Silber, M. A. Biasutti, E. Abuin and E. Lissi, *Adv. Colloid Interface Sci.*, 1999, **82**, 189.
3 S. P. Moulik and B. K. Paul, *Adv. Colloid Interface Sci.*, 1998, **78**, 99.
4 N. Nandi, K. Bhattacharyya and B. Bagchi, *Chem. Rev.*, 2000, **100**, 2013.
5 J. Eastoe and S. Gold, *Phys. Chem. Chem. Phys.*, 2005, **7**, 1352.
6 V. Uskokovic and M. Drofenik, *Adv. Colloid Interface Sci.*, 2007, **133**, 23.
7 N. M. Correa, M. A. Biasutti and J. J. Silber, *J. Colloid Interface Sci.*, 1995, **172**, 71.
8 N. M. Correa, M. A. Biasutti and J. J. Silber, *J. Colloid Interface Sci.*, 1996, **184**, 570.
9 D. Grand and A. Dokutchaev, *J. Phys. Chem. B*, 1997, **101**, 3181.
10 M. B. Costa and R. L. Brookfield, *J. Chem. Soc., Faraday Trans. 2*, 1986, **82**, 991.
11 M. Vasilescu, A. Caragheorgheopol and H. Caldararu, *Adv. Colloid Interface Sci.*, 2001, **89**, 169.
12 S. S. Quintana, R. D. Falcone, J. J. Silber and N. M. Correa, *ChemPhysChem*, 2012, **13**, 115.
13 O. Myakonkaya and J. Eastoe, *Adv. Colloid Interface Sci.*, 2009, **149**, 39.
14 M. D. Fayer and N. E. Levinger, *Annu. Rev. Anal. Chem.*, 2010, **3**, 89.
15 N. M. Correa, R. D. Falcone, M. A. Biasutti and J. J. Silber, *Langmuir*, 2000, **16**, 3070.
16 R. D. Falcone, N. M. Correa and J. J. Silber, *Langmuir*, 2009, **25**, 10426.
17 R. D. Falcone, B. Baruah, E. Gaidamauskas, C. D. Rithner, N. M. Correa, J. J. Silber, D. C. Crans and N. E. Levinger, *Chem.–Eur. J.*, 2011, **17**, 6837.
18 N. M. Correa, J. J. Silber, R. E. Riter and N. E. Levinger, *Chem. Rev.*, 2012, **112**, 4569.
19 D. D. Ferreyra, N. M. Correa, J. J. Silber and R. D. Falcone, *Phys. Chem. Chem. Phys.*, 2012, **14**, 3460.
20 R. McNeil and J. K. Thomas, *J. Colloid Interface Sci.*, 1981, **83**, 57.
21 A. Jada, J. Lang, R. Zana, R. Makhloufi, E. Hirsch and S. J. Candau, *J. Phys. Chem.*, 1990, **94**, 387.
22 M. S. Baptista and C. D. Tran, *J. Phys. Chem. B*, 1997, **101**, 4209.
23 D. Grand, *J. Phys. Chem. B*, 1998, **102**, 4322.
24 S. S. Quintana, F. Moyano, R. D. Falcone, J. J. Silber and N. M. Correa, *J. Phys. Chem. B*, 2009, **113**, 6718.
25 F. Moyano, R. D. Falcone, J. C. Mejuto, J. J. Silber and N. M. Correa, *Chem.–Eur. J.*, 2010, **16**, 8887.
26 P. R. Majhi and S. P. Moulik, *J. Phys. Chem. B*, 1999, **103**, 5977.
27 S. K. Hait, A. Sanyal and S. P. Moulik, *J. Phys. Chem. B*, 2002, **106**, 12642.
28 E. Abuin, E. Lissi, R. Duarte, J. J. Silber and M. A. Biasutti, *Langmuir*, 2002, **18**, 8340.
29 L. García Rios, A. Godoy and P. Rodriguez-Dafonte, *Eur. J. Org. Chem.*, 2006, **15**, 3364.
30 A. Jada, J. Lang and R. Zana, *J. Phys. Chem.*, 1990, **94**, 381.
31 A. Salabat, J. Eastoe, K. J. Mutch and R. F. Tabor, *J. Colloid Interface Sci.*, 2008, **318**, 244.
32 O. Myakonkaya, J. Eastoe, K. J. Mutch, S. Rogers, R. Heenan and I. Grillo, *Langmuir*, 2009, **25**, 2743.
33 M. J. Hollamby, R. Tabo, K. J. Mutch, K. Trickett, J. Eastoe, R. K. Heenan and I. Grillo, *Langmuir*, 2008, **24**, 12235.
34 F. M. Agazzi, R. D. Falcone, J. J. Silber and N. M. Correa, *J. Phys. Chem. B*, 2011, **115**, 12076.
35 B. Lemaire, P. Bothorel and D. Roux, *J. Phys. Chem.*, 1983, **87**, 1023.
36 F. M. Agazzi, J. Rodriguez, R. D. Falcone, J. J. Silber and N. M. Correa, *Langmuir*, 2013, **29**, 3556.
37 F. M. Agazzi, N. M. Correa and J. Rodriguez, *Langmuir*, 2014, **30**, 9643.
38 P. G. Molina, J. J. Silber, N. M. Correa and L. Sereno, *J. Phys. Chem. C*, 2007, **111**, 4269.

39 J. S. Florez Tabares, M. L. Blas, L. E. Sereno, J. J. Silber, N. M. Correa and P. G. Molina, *Electrochim. Acta*, 2011, **56**, 10231.
40 F. Moyano, P. G. Molina, J. J. Silber, L. Sereno and N. M. Correa, *ChemPhysChem*, 2010, **11**, 236.
41 I. D. Charlton and A. P. Doherty, *Electrochem. Commun.*, 1999, **1**, 176.
42 Malvern Instruments, Technical Note, http://www3.nd.edu/~rroeder/ame60647/slides/dls.pdf.
43 J. T. Schrodt and R. M. Akel, *J. Chem. Eng. Data*, 1989, **34**, 8.
44 M. Fleishmann, S. Pons, D. R. Rolinson and P. P. Schmidt, in *Ultramicroelectrodes*, Datatech Systems, North Carolina, 1987.
45 C. Barbero, M. A. Zon and H. Fernandez, *J. Electroanal. Chem.*, 1989, **265**, 23.
46 A. J. Bard and L. R. Faulkner, in *Electrochemical Methods: Fundamentals and Applications*, Wiley, NY, 2nd edn, 2001.
47 C. Petit, A. S. Bommarius, M. P. Pileni and T. A. Hatton, *J. Phys. Chem.*, 1992, **96**, 4653.
48 H. Matsuda and Y. Ayabe, *Z. Elektrochem.*, 1955, **59**, 494.
49 Z. Galus, J. Golas and J. Osteryoung, *J. Phys. Chem.*, 1988, **92**, 1103.
50 J. B. Flanagan, S. Margel, A. J. Bard and F. C. Anson, *J. Am. Chem. Soc.*, 1978, **100**, 4248.
51 S. S. Atik and J. K. Thomas, *J. Am. Chem. Soc.*, 1981, **103**, 3543.
52 D. G. Scott, *Nature*, 1960, **188**, 908.
53 G. D. Scott and D. M. Kilgour, *Br. J. Appl. Phys.*, 1969, **2**, 863.
54 R. D. Kamien and A. J. Liu, *Phys. Rev. Lett.*, 2007, **99**, 155501.
55 R. S. Farr and R. D. Groot, *J. Chem. Phys.*, 2009, **131**, 244104.